


ORIGINAL ARTICLE

Open Access



Relationship between Hardness and Deformation during Cold Rolling Process of Complex Profiles

Dawei Zhang^{1*} , Linghao Hu¹, Bingkun Liu¹ and Shengdun Zhao¹

Abstract

The hardening on surface of complex profiles such as thread and spline manufactured by cold rolling can effectively improve the mechanical properties and surface quality of rolled parts. The distribution of hardness in superficial layer is closely related to the deformation by rolling. To establish the suitable correlation model for describing the relationship between strain and hardness during cold rolling forming process of complex profiles is helpful to the optimization of rolling parameters and improvement of rolling process. In this study, a physical analog experiment reflecting the uneven deformation during complex-profile rolling process has been extracted and designed, and then the large data set (more than 400 data points) of training samples reflecting the local deformation characteristics of complex-profile rolling have been obtained. Several types of polynomials and power functions were adopted in regression analysis, and the regression correlation models of 45# steel were evaluated by the single-pass and multi-pass physical analog experiments and the complex-profile rolling experiment. The results indicated that the predicting accuracy of polynomial regression model is better in the strain range (i.e., $\varepsilon < 1.2$) of training samples, and the correlation relationship between strain and hardness out strain range (i.e., $\varepsilon > 1.2$) of training samples can be well described by power regression model; so the correlation relationship between strain and hardness during complex-profile rolling process of 45# steel can be characterized by a segmented function such as third-order polynomial in the range $\varepsilon < 1.2$ and power function with a fitting constant in the range $\varepsilon > 1.2$; and the predicting error of the regression model by segmented function is less than 10%.

Keywords Complex profile, Cold rolling, Multi passes, Equivalent strain, Vickers hardness

1 Introduction

Cold rolling is an efficient and accurate bulk forming technology for shaft parts with complex characteristics such as thread and spline, which has the high precision, good mechanical properties, high productivity and high material availability compared with the traditional cutting process [1–5]. The work-hardening phenomenon

is notable in cold plastic forming of metals, and the strength and hardness increase after plastic deformation. For example, the hardness of parts manufactured by thread rolling with round die [6], spline rolling with round die [7], thread rolling with flat die [8], helical gear rolling with flat die [9] changes significantly from the surface to the core, and the hardness in superficial layer increases significantly. However, the hardness in superficial layer of machined thread [6] and helical gear [9] is almost unchanged.

The performance of metal will be improved by plastic forming process [10], especially the cold work hardening increasing strength. The hardness of metal reflects the resistance to micro local deformation [11], and is one of

*Correspondence:

Dawei Zhang
zhangdawei2000@mail.xjtu.edu.cn

¹ Xi'an Key Laboratory of Intelligent Equipment and Control, School of Mechanical Engineering, Xi'an Jiaotong University, Xi'an 710049, China

important properties of materials. It is generally believed that there is a positive correlation between material hardness and material strength (such as tensile strength and yield strength). Many scholars have devoted themselves to studying the relationship between the strength and hardness. Based on the stress-strain relationship described by the power function (Eq. (1)), the relationship between yield strength and hardness (Eq. (2)) [12] and the relationship between tensile strength and hardness (Eq. (3)) [13] have been deduced.

$$\sigma = b_{E1}\varepsilon^n, \quad (1)$$

where b_{E1} is a constant; n is the hardening index.

$$\sigma_Y = \frac{H_V}{3}(b_{E2})^n, \quad (2)$$

$$\sigma_T = \frac{H_V}{2.9}\left(\frac{n}{0.217}\right)^n, \quad (3)$$

where σ_Y is the yield strength; H_V is the Vickers diamond pyramid hardness number; b_{E2} is a constant; σ_T is the tensile index.

Pavlina and Van Tyne [14] declared that the yield strength and tensile strength are linearly related to the hardness for steel with higher strength such as $\sigma_Y \in (300 \text{ MPa}, 1700 \text{ MPa})$ and $\sigma_T \in (450 \text{ MPa}, 2350 \text{ MPa})$, which can be expressed by Eq. (4). For electroformed nanocrystalline material [15] and irradiated steels [16], Eq. (5) can be used to describe the linear relationship between yield strength or tensile strength and hardness.

$$\sigma_{Y,T} = a_{E4} + b_{E4}H, \quad (4)$$

where a_{E4} and b_{E4} is the constants; H is the hardness.

$$\sigma_{Y,T} = b_{E5}H, \quad (5)$$

where b_{E5} is a constant.

Most of above studies have been used to evaluate the material performance. Moreover, some scholars established the predicted model of hardness based on the microstructure, such as the relationship between grain size [17] or dislocation density [18] between hardness. However, the relationship between grain size or dislocation density between stress was established firstly, and then the relationship between stress and hardness was established. For regression analysis for initial grain size and hardness, the training samples is too small. It is difficult to obtain precise dislocation density by numerical simulation.

Tabor [11] declared that the hardness of material is linearly related to flow stress, and the hardness is also closely related to strain. The prediction and collection of strain during plastic forming process are pretty

mature by means of numerical simulation. The predicting model considered deformation can be convenient for engineering application. The constitutive model of material deformed at room temperature can be described by power function such as Eq. (1), so power function such as Eq. (6) is also able to describe the correlation between strain and hardness [8]. Kim et al. [19] acquired the data of strain and hardness by using cylindrical compression test, where the strain is obtained by finite element method (FEM), and then the modified power function such as Eq. (7) was fitted base on the data of strain and hardness. Where the strain of training data is 0–1.2, and the fitted relationship model has been use to predict the distribution of strain in cold extrusion process.

$$H_V = b_{E6}\varepsilon^x, \quad (6)$$

where b_{E6} is a constant; x is the Meyer index.

$$H_V = a_{E7} + b_{E7}\varepsilon^x, \quad (7)$$

where a_{E7} and b_{E7} are the constants.

In order to make predicting model of hardness be more universal, some scholars also tried to establish a predicting model included material constants. Based on the Brinell hardness test and Vickers hardness test, Sonmez and Demir [20] established an analytical model for hardness calculation including material constants such as b_{E1} and n in Eq. (1), and then to attach strain to construct a hardness-strain correlation model. The maximum predicting error for Brinell hardness (H_B) and Vickers hardness (H_V) by using the analytical model before attaching strain are 15.2% and 18%, respectively, although the average prediction error is 5.6%. However, the description of hardness-strain data in Refs. [19, 21] by using the hardness-strain correlation model after attaching strain in Ref. [20] was worse than the empirical model in Refs. [19, 21].

By using cylindrical compression test with a near frictionless, the strain data were obtained and the hardness data were measured in core of corresponding compressed cylinder by Gouveia et al. [21], and then the relationship between hardness and strain was described by a second-order polynomial (Eq. (8)). Where the strain of training data is 0–1, and the regression model has been use to evaluate the deformation according to the hardness of cold extruded part. Narayanan et al. [22] extracted the data of strain and hardness in cold forming process of pure aluminum under four lubricated conditions ($m = 0.16\text{--}0.33$) by using the method in Ref. [19]. The relationship between hardness and strain was described by a first-order polynomial ($c_{E8} = 0$ in Eq. (8)), the regression polynomial was used in analysis of extrusion process. The results indicated that the regression polynomial

is more suitable for describing the strain-hardness relationship under lubrication conditions of $m=0.16-0.25$.

$$H_V = a_{E8} + b_{E8}\varepsilon + c_{E8}\varepsilon^2, \quad (8)$$

where a_{E8} , b_{E8} and c_{E8} are the constants.

For complex-profile rolling process, Eq. (6) was used to describe the relationship between equivalent strain and Vickers hardness by Chen et al. [23], and training samples such as hardness and strain data were taken from the cylindrical compression test. The modified power function (Eq. (7)) was used to describe the relationship between equivalent strain and Vickers hardness by Domblesky and Feng [8], and then the Vickers hardness distribution of cold thread rolling with flat die was calculated by the modified power model according to the strain field data obtained by the FEM results. The modified power function (Eq. (7)) was also used to describe the relationship between equivalent strain and Vickers hardness by Kamouneh et al. [9], and strain distribution of gear rolling with flat die was calculated by the modified power model according to Vickers hardness measured by experiment.

However, the deformation in complex-profile rolling process is a typical local loading deformation, the deformation zone is concentrated on the superficial layer, and the degree of deformation is also less than that in extrusion and forging processes. The simple cylindrical compression test cannot reflect the deformation characteristics in complex-profile rolling process. Up to now, for the hardness-strain correlation model used in cold rolling process, the research in Refs. [8, 9] did not report the scale and strain-range of training-sample data; and there are only 28 training samples in the research in Ref. [23], and the strain of training samples was about 0.2–1. However, the predicted strain in superficial layer was about 0.04–1.41 in thread rolling with flat die [8] and is about 0.1–0.9 in helical gear rolling with flat die [9]. In addition, the relevant parameters in the correlation model for different materials are quite different, as listed in Table 1. It is necessary to further study correlation between the hardness and deformation for reflecting the

forming characteristics of complex-profile rolling under a larger strain-range, more training-sample data and specified material.

Therefore, in this study, a physical analog experiment (PAE) reflecting the uneven deformation during complex-profile rolling process has been extracted and designed, and the data (more than 400 data points) of hardness and matching strain have been obtained based on a combination of physical analog experiment and finite element analysis (FEA). The polynomial and power function regressions were used to correlation model between hardness and strain for complex rolling process of 45# steel (i.e., AISI 1045). The testing samples, i.e., verifying samples, were obtained from single-pass and multi-pass PAEs. Three polynomial regression models and three power function regression models were evaluated by the verifying samples, significance test of regression equation, and significance test of regression coefficient. The results indicated that the segmented function combined third-order polynomial and power function with a fitting constant can be used to describe the relationship between strain and hardness in cold rolling process of complex profile.

2 Complex-profile Rolling and Its Analog Experiment

Generally, rolling process with round die of complex profiles such as splines and threads can be divided into radial feed rolling and axial feed rolling, and two or three rolling dies are often used. In the two types of rolling processes, the rolling die has the same rotational movement, and the direction of rotation for workpiece is opposite to that for rolling die. However, there is no relative axial movement between the die and the workpiece during the radial feed rolling process, and there is relative axial movement between the die and the workpiece during the axial feed rolling process.

In complex-profile rolling process, the radial compression into the workpiece by rolling die increases gradually, and the profile of the workpiece gradually

Table 1 Regression parameters

Material	Power function			Polynomial			Refs.
	a_{E7}	b_{E6} or b_{E7}	x	a_{E8}	b_{E8}	c_{E8}	
AISI 4620	180	151	1.6	–	–	–	[9]
AISI 1018	190	95	0.41	–	–	–	[8]
AISI 1010	102.8	84.9	0.4	–	–	–	[19]
AISI 302	0	387.64	0.38	–	–	–	[23]
WNr 1.0303	–	–	–	115.1	119.1	–60.7	[21]
Pure aluminum	–	–	–	74.5	29.15	0	[22]

forms. In radial feed rolling, the radial compression of rolling die is the same along axial direction, and the profile of the workpiece is also the same along axial direction. The radial compression can be realized by the radial movement of rolling die, as shown in Figure 1(a); or the rolling die has no infeed movement, but its height of profile changes along the circumferential direction. In axial feed rolling, the radial compression of rolling die is different along axial direction, and the profile of the workpiece is also different along axial direction. Generally, the rolling die has an entry-angle, and the radial compression of rolling die gradually increases along direction of axial feed in entry-angle section, as shown in Figure 1(b).

Although the profile of spline is different from the profile of thread, and the radial compression of rolling die and profile of workpiece are both different along the axial direction, the formation process of splined profile on cross section is similar to that of threaded profile on axial section, as shown in Figure 2(a) and (b). The deformations are also similar, that is, the deformation in bottom of profile is greater than that in flank of profile, and deformation in the flank is greater than that in top of profile. Therefore, according to the shape characteristics and the deformation characteristics, a physical analog experiment has been designed, as shown in Figure 3(a). The upper die similar to the splined and threaded profile is pressed into the blank to form a profile similar to the rolled complex profile, as shown in Figure 2(c). The similar experiment was also used to study the convex at root in spline rolling process by Zhang and Zhao [24], but the width direction of the blank is strongly restrained, which is greater than the circumferential restraint in the rolling process. In order to further simulate the local loading state in the complex-profile rolling process, and considering the

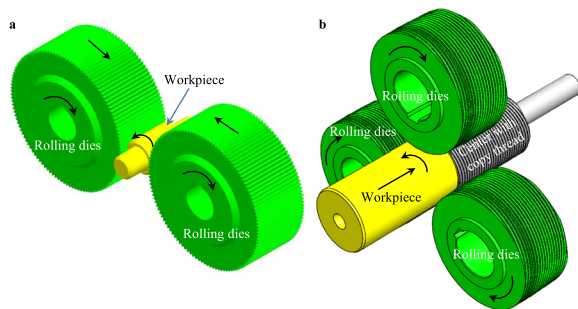


Figure 1 Sketch of complex-profile rolling process: (a) Spline rolling with infeed, (b) Thread rolling with axial feed

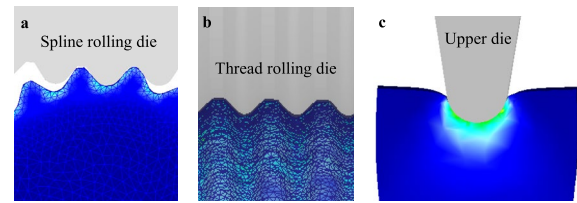


Figure 2 Shape characteristic in complex-profile rolling: (a) Spline rolling, (b) Thread rolling, (c) Physical analog experiment

capacity of testing machine, the blank is placed on the flat die without other constraints in this study.

An experimental platform of PAE was constructed based on the 100 kN Instron electronic universal testing machine, as shown in Figure 3(b). The material of the upper and lower dies is T8 steel, and the material of workpiece is 45# steel. The power function (Eq. (1)) is used to describe the relationship between stress and strain for 45# steel in cold plastic deformation, which can be expressed as Eq. (9) [25] according to the uniaxial tensile test data:

$$\sigma = 1450(0.0132715 + \varepsilon)^{0.2817}. \tag{9}$$

According to Eq. (9), size of upper die and capacity of machine, the blank in the PAE was 16 mm in length, 12 mm in width and 15 mm in height, and the upper die stroke is 2 mm. Oil lubrication was used in PAE. Under these geometrical and processing parameters, the maximum forming load is about 99.5 kN predicted by FEA, and PAE can be carried out by the Instron electronic universal testing machine. The experiment result was shown in Figure 3(c).

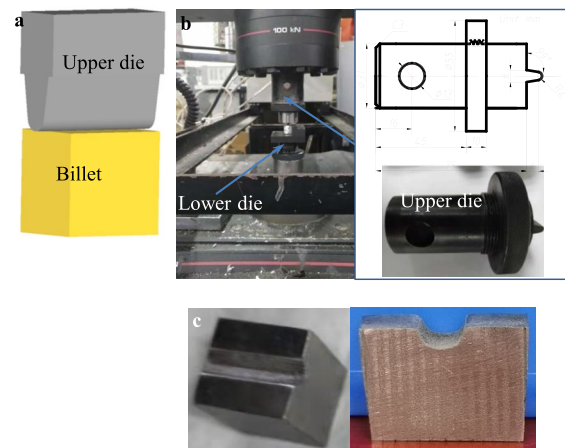


Figure 3 Physical analog experiment: (a) Principle, (b) Experimental apparatus, (c) Experimental result

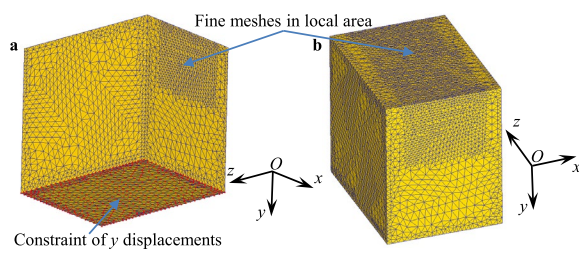


Figure 4 Boundary constraint and meshes for workpiece: (a) Constraint of lower surface, (b) Initial mesh

3 Data Extraction of Hardness and Strain

Based on DEFORM code, a 3D-FE model of PAE process has been developed. During forming process of PAE, the function of lower die is only to constrain the y displacements on the lower surface of workpiece, where the y direction is the loading direction of upper die. Thus, the FE model can only include the upper die and workpiece, as shown in Figure 3(a). The constraint of lower die can be realized by boundary condition of FE model, such as the constraint of y displacements for the lower surface of workpiece, as shown in Figure 4(a).

The workpiece is a deformable body, and the elastic deformation can be ignored in analysis of bulk metal forming process, so the workpiece can be considered as a plastic body in the FE model. The yielding behavior of deformable metal meets Mises yield criterion. Eq. (9) was used to describe the stress-strain relationship of the workpiece. The stiffness and strength of die are much larger than those of workpiece, so the die can be considered as a rigid body in the FE model.

According to the geometric parameters of the die and workpiece in Section 2, the geometric model was built, and the local refinement and remeshing technology was adopted for the meshing of the workpiece. 50000 elements were adopted, and the initial minimum mesh size was about 0.127 mm. The area to form profile has a fine mesh, as shown Figure 4(b).

Friction between die and workpiece is an important boundary condition and influencing factor for metal forming process. The reasonable frictional model and its parameter are the key to describe the frictional behavior [26, 27]. Because of the simplification and numerical rigidity, shear friction model is often used in finite element analysis of bulk metal forming process [28–31]. The incremental ring compression test can reflect the lubrication characteristics in complex-profile rolling, the shear friction factor $m = 0.21$ under oil lubrication was determined by the incremental ring compression test [25]. Thus, $m = 0.21$ was adopted in the FEA.

The FEA results (Figure 5(a)) and experimental results (Figure 3(c)) indicated that there are slight protrusions at the profiled bottoms at both ends after deformation, and there is a certain axial displacement during the forming process. However, the maximum axial (i.e., Z direction) displacement (0.66–0.88 mm) is only in the local area of the protrusion, and the axial displacement in most areas is small. This was consistent with the phenomenon of convex at root of spline by rolling forming [24], and the protrusion/convex only affects the shape of profile in a small range of the free end face. Therefore, the hardness test was performed on the axial symmetrical section of the workpiece, i.e., the section with zero axial displacement in Figure 5(a), and the strain information was extracted from the section based on FEA result.

Figure 5(b) illustrates that distributing characteristics of strain on this section, and indicates that the deformation is concentrated in the superficial area of the workpiece, which is consistent with the deformation characteristics of thread rolling process and spline rolling process. Taking 40 points along the profiled groove to analyze the distribution of strain, as shown in Figure 5(c). The equivalent strain in top of profile is small, and then gradually increases along the flank of profile from top to bottom, and the equivalent strain in bottom of profile is the largest. There are certain differences of bottom and flank zones between PAE and thread or spline rolling. Such as involute flank or helical flank is presented in spine rolling process or thread

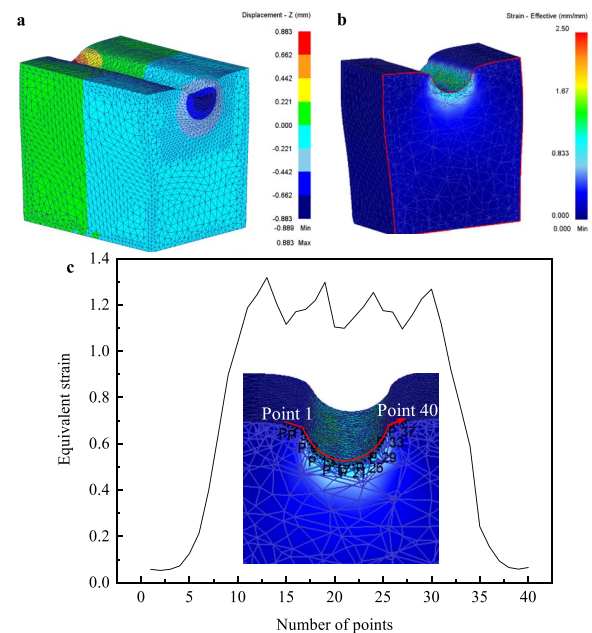


Figure 5 FEA results of PAE: (a) Distribution of displacement, (b) Distribution of strain, (c) Distribution of strain on surface

rolling process, respectively, but a line-flank is adopted in PAE. However, from the perspective of geometry, the bottom and flank in PAE are similar to the circular root of workpiece in thread or spline rolling process. The deformation inhomogeneity in the bottom, flank and top/crest zones in PAE is also similar to that in thread or spline rolling process.

The deformed sample by PAE was cut at the axial symmetrical section of the workpiece, and the section was polished to meet the measurement requirements, and the low-load Vickers hardness test (HV0.5) has been carried out with 500 g maintaining for 15 s. The hardness test was performed on the five positions/lines, such as OC_L , OF_L , OR, OC_R and OF_R , as shown in Figure 6(a), which can reflect the deformation characteristic in bottom/root, flank and top/crest zones along y /radial direction. One point was taken every 0.1 mm from the surface to the inside along vertical direction (y axis) until the hardness of the neighboring five points being almost the same. In addition, the low-load Vickers hardness test was also performed at the position in the non-deformation zone near the bottom, such as OO shown in Figure 6(a). Figure 6(b) illustrates the distribution of hardness on the symmetrical section. Where, the hardness shown in rectangular box is the average

value of several points in the rectangular box due to the large number of measured data.

The measured hardness at the OO position can be regarded as the initial hardness of the undeformed 45# steel, which is about 180 HV. The distributing characteristics of hardness for OC_L and OC_R are basically the same, and these for OF_L and OF_R are also the same basically, as shown in Figure 6(c). The order of the hardness values (DPH) of the five positions with the same y coordinate is $DPH(OR) > DPH(OFL,R) > DPH(OC_{L,R})$. However, the difference of hardness among the five lines decreases as y increases, and the hardness for OC_L , OF_L , OR, OC_R and OF_R tends to be the same after a certain y value, which is about 190 HV. The hardness in superficial layer of workpiece from PAE is about 260–310 HV.

Figure 7 illustrates the distribution of strain along y axis for five lines such as OC_L , OF_L , OR, OC_R and OF_R . The distributing and changing characteristics of strain for the five lines are almost the same as those of the hardness. The hardness and equivalent strain for bottom such as OR and flank such as OF_L and OF_R increase with decreasing y , and the hardness and equivalent strain for top/crest such as OC_L and OC_R increase firstly and then decrease with decreasing y . Those also proved that there is a certain positive correlation between hardness and equivalent strain. According to the FEA results, the equivalent strain at the same position as the hardness test has been extracted. More than 400 data points, such as 407 data points, were obtained, as shown in Figure 8, and the strain is from 0 to 1.2.

In spline or thread rolling process, the deformation decreases from in bottom/root zone to flank zone, and to top/crest zone. The stress and strain decrease form root to flank and to crest in thread rolling process [32]. The deformation degree decrease from root zone to flank in

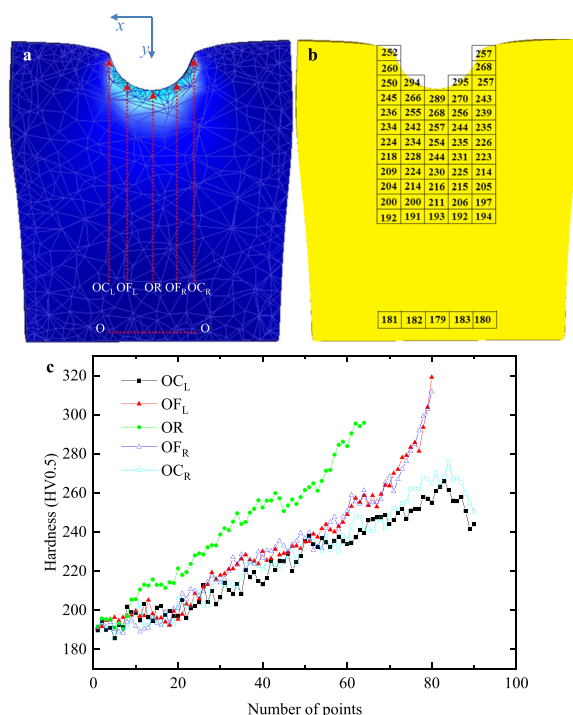


Figure 6 Extraction of Vickers hardness: (a) Measured location, (b) Distribution of hardness on the section, (c) Distribution of hardness along radial (y) direction

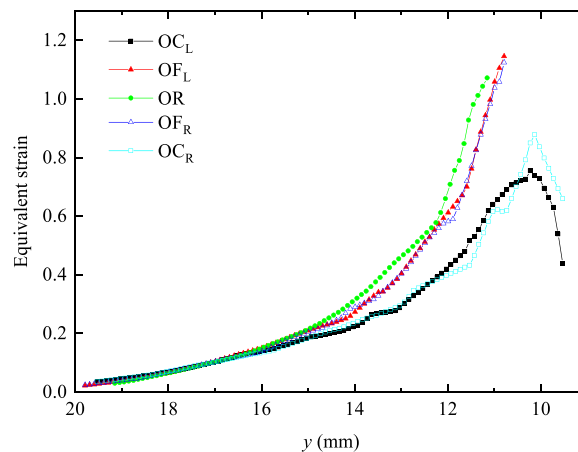


Figure 7 Distribution of strain along selected lines

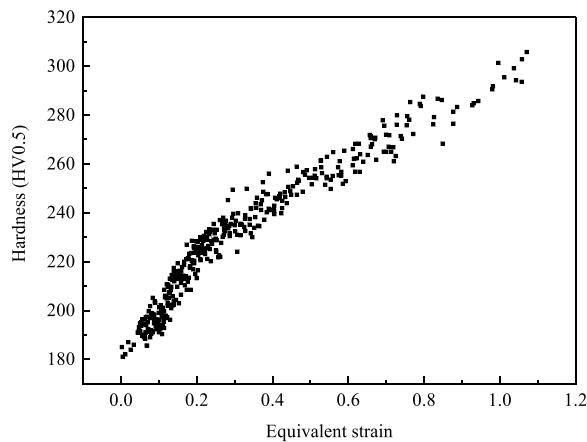


Figure 8 Scatter plot of strain-hardness

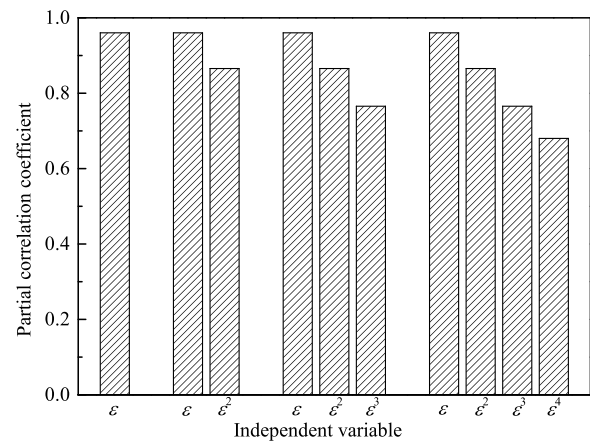


Figure 9 Partial correlation coefficient of regression coefficient

spline rolling process [33]. The hardness in OC_L and OC_R also increase firstly and then decrease with decreasing y , shown in Figure 6. This also indicated that the deformation in OC_L and OC_R also increase firstly and then decrease with decreasing y . In the spline rolling process, the hardness also increases firstly and then decrease along radial direction [7]. The OC_L and OC_R in PAE reflect the deformation characteristic in top/crest zone along y /radial direction, and thus strain along OC_L and OC_R presents the increase firstly and then decrease with decreasing y in Figure 7.

4 Correlation Model between Hardness and Deformation

Up to now, the polynomial and power models are mostly used in the description of the relationship between strain and hardness. The polynomial model and power model also contain multiple types. Based on the relevant data collected in Section 3, using statistical analysis methods and combining experimental data, multi types of correlation models for hardness and deformation are discussed, and predicting model of hardness suitable for 45 steel in cold rolling process has been determined.

4.1 Polynomial Regression Model

The regression fitting is performed by the least square method, and the data shown in Figure 8 are fitted by the first to fourth-order polynomials, respectively. The regression models can be expressed by Eqs. (10, 11, 12, 13):

$$H_{V, \text{poly1}} = 193.9 + 112.1\varepsilon, \tag{10}$$

$$H_{V, \text{poly2}} = 183.9 + 185\varepsilon - 81.3\varepsilon^2, \tag{11}$$

$$H_{V, \text{poly3}} = 175.7 + 280\varepsilon - 324.3\varepsilon^2 + 162.9\varepsilon^3, \tag{12}$$

$$H_{V, \text{poly4}} = 173.3 + 319.7\varepsilon - 499.7\varepsilon^2 + 433.7\varepsilon^3 - 132.7\varepsilon^4. \tag{13}$$

The correlation coefficient test and statistical hypothesis test were carried out on the above regression equation for significance test. The results indicated that the multiple correlation coefficients R are 0.9602, 0.9784, 0.9842 and 0.9845, respectively, which are all greater than the critical value R_α of multiple correlation coefficient under $\alpha = 0.01$, so the regression equation is significant. In the statistical hypothesis test, the variance ratio F of the regression equation is also much larger than the critical value F_α under $\alpha = 0.01$, and the four regression equations are highly significant.

The regression coefficient significance test was also carried out for polynomial regression models Eqs. (10, 11, 12, 13). The partial correlation coefficient V_j is used to check the significance of the regression coefficient. Figure 9 illustrates the partial correlation coefficients of regression coefficient in Eqs. (10, 11, 12, 13). Where, the partial correlation coefficients are between 0.6803 and 0.9602, and the order of independent variables affecting the dependent variable such as hardness is $\varepsilon > \varepsilon^2 > \varepsilon^3 > \varepsilon^4$. The t -test on Eqs. (10, 11, 12, 13) has been performed under the confidence level of $\alpha = 0.01$. The results indicated that the absolute value of t -test for the constant and independent variables of Eqs. (10, 11, 12) are greater than the critical value, but the absolute value of the t -test the highest order term (ε^4) in fourth-order polynomial such as Eq. (13) is less than the critical value and should be eliminated. Significance tests based on regression coefficients showed that polynomials (Eqs.

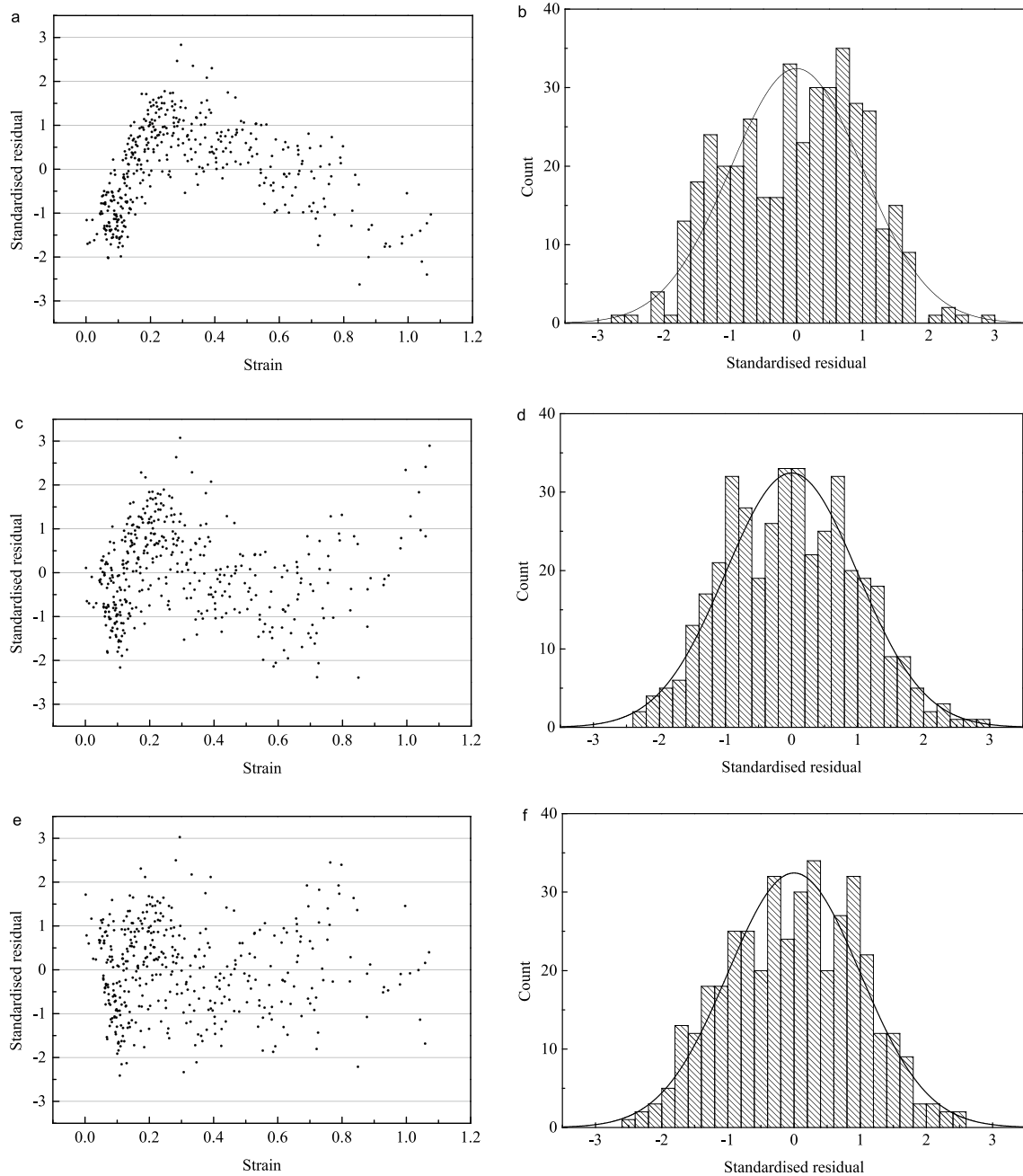


Figure 10 Normal frequency and distribution of residual for polynomial regression equation: (a) Residual normal frequency of first-order polynomial, (b) Residual distribution of first-order polynomial, (c) Residual normal frequency of second-order polynomial, (d) Residual distribution of second-order polynomial, (e) Residual normal frequency of third-order polynomial, (f) Residual distribution of third-order polynomial

(10, 11, 12)) of the first to third-order are suitable for describing the correlation between hardness and strain.

The residual analysis for regression equations Eqs. (10, 11, 12) were carried out. Figure 10 illustrates the normal frequency test of the residuals. It can be found from Figure 10(a) that 97.30% of the standardized residuals of the first-order regression model (Eq. (10)) fall within the (−2,

2) interval; and it also can be found from Figure 9(c) and (e) that 96.31% and 96.56% of the standardized residuals for second-order (Eq. (11)) and third-order (Eq. (12)) regression models fall within the (−2, 2) interval. The assumption of normal distribution of errors for the polynomial regression model (Eqs. (10, 11, 12)) is reasonable. Furthermore, it can be seen from Figure 10(b), (d), and

(f) that the residuals obey a normal distribution and conform to the assumption of polynomial regression.

The outliers whose standardized residuals are outside the $(-2, 2)$ interval were eliminated according to Figure 10. The data eliminating outliers have been fitted by the first to third-order polynomials, respectively. The regression models can be expressed by Eqs. (14, 15, 16). Compared with Eqs. (10, 11, 12), only the fitting coefficients are slightly different. The multiple correlation coefficients R of the regression equations are 0.9641, 0.9816 and 0.9866, respectively, which are all greater than the critical value of the multiple correlation coefficient under $\alpha = 0.01$, and greater than the corresponding R of Eqs. (10, 11, 12). Similarly, the variance ratio F of Eqs. (14, 15, 16) is much larger than the critical value under $\alpha = 0.01$, and it is significantly greater than the corresponding F of the regression equation before eliminating outliers. All these indicated that the significant of the polynomial regression equation after removing the outliers has been obviously improved.

$$H_{V, \text{poly1}} = 193.4 + 113.7\varepsilon, \quad (14)$$

$$H_{V, \text{poly2}} = 183.2 + 189.9\varepsilon - 87.42\varepsilon^2, \quad (15)$$

$$H_{V, \text{poly3}} = 176 + 277.2\varepsilon - 319.9\varepsilon^2 + 161.1\varepsilon^3. \quad (16)$$

The regression coefficient significance test was also carried out for polynomial regression model Eqs. (14, 15, 16). The results also indicated that the partial correlation coefficients of the independent variables were all greater than the corresponding V_j before eliminating outliers. The $|t_j|$ in t -test of constant and independent variables for Eqs. (14, 15, 16) also increased, and all are greater than the critical value. These indicated that the effect of independent variables of the polynomial regression equation after removing outliers on the significance of the dependent variables has been obviously improved.

4.2 Power Regression Model

Two derivative forms Eq. (17) and Eq. (18) can be obtained from Eq. (7):

$$H_V = H_{V, \text{initial}} + b_{E17}\varepsilon^x, \quad (17)$$

where $H_{V, \text{initial}}$ is initial hardness of metal; b_{E17} is a constant,

$$H_V = b_{E18}(\varepsilon + a_{E18})^x, \quad (18)$$

where a_{E18} and b_{E18} are the constants.

The data shown in Figure 8 are fitted by power function (Eq. (6)) without constant term, power function (Eq. (17)) with the initial hardness as constant, and

power function (Eq. (18)) with a fitting constant. The regression models can be expressed by Eqs. (19, 20, 21), where the initial hardness of the material is 180HV according to the analysis in Section 3.

$$H_{V, \text{powerF}} = 227.186\varepsilon^{0.1334}, \quad (19)$$

$$H_{V, \text{powerS}} = 180 + 132.3\varepsilon^{0.8175}, \quad (20)$$

$$H_{V, \text{powerT}} = 284.8(\varepsilon + 0.095)^{0.2126}. \quad (21)$$

In order to do significance test for regression equation and regression coefficient, the linearization and change of variable have been carried out for Eqs. (19, 20, 21). Then, correlation coefficient test and statistical hypothesis test were carried out on the above regression equation for significance test. The results indicated that the multiple correlation coefficients R are 0.9478, 0.9538 and 0.9819, and are all greater than the critical value R_α of the multiple correlation coefficient under $\alpha = 0.01$, so the regression equation is significant. In the statistical hypothesis test, the variance ratio F of the regression equation is also much larger than the critical value F_α under $\alpha = 0.01$.

The regression coefficient significance test was also carried out for the linearized power regression equations. The partial correlation coefficients of the independent variables for three linearized equations are 0.9478, 0.9538 and 0.9819, respectively. The t -test with confidence level of $\alpha = 0.01$ also indicated that the absolute value of t -test for the constant and independent variables are much greater than the critical value. Significance tests based on regression equation and regression coefficient indicated that three power regression models (Eqs. (19, 20, 21)) are also suitable for describing the correlation between hardness and strain.

The residual analysis for the linearized power regression equations were also carried out. Figure 11 illustrates the normal frequency test of the residuals. It can be found that 98.03% of standardized residuals of power regression model without a constant term fall within the $(-2, 2)$ interval, as show in Figure 11(a); 95.58% of standardized residuals of power regression model with initial hardness fall within the $(-2, 2)$ interval, as shown in Figure 11(c); 96.56% of standardized residuals of power regression model with a fitting constant fall within the $(-2, 2)$ interval, as shown in Figure 11(e). The assumption of normal distribution of errors in the power regression models (Eqs. (19, 20, 21)) is reasonable. Furthermore, it can be seen from Figure 11(b), (d), and (f) that the residuals obey a normal distribution and conform to the regression assumption.

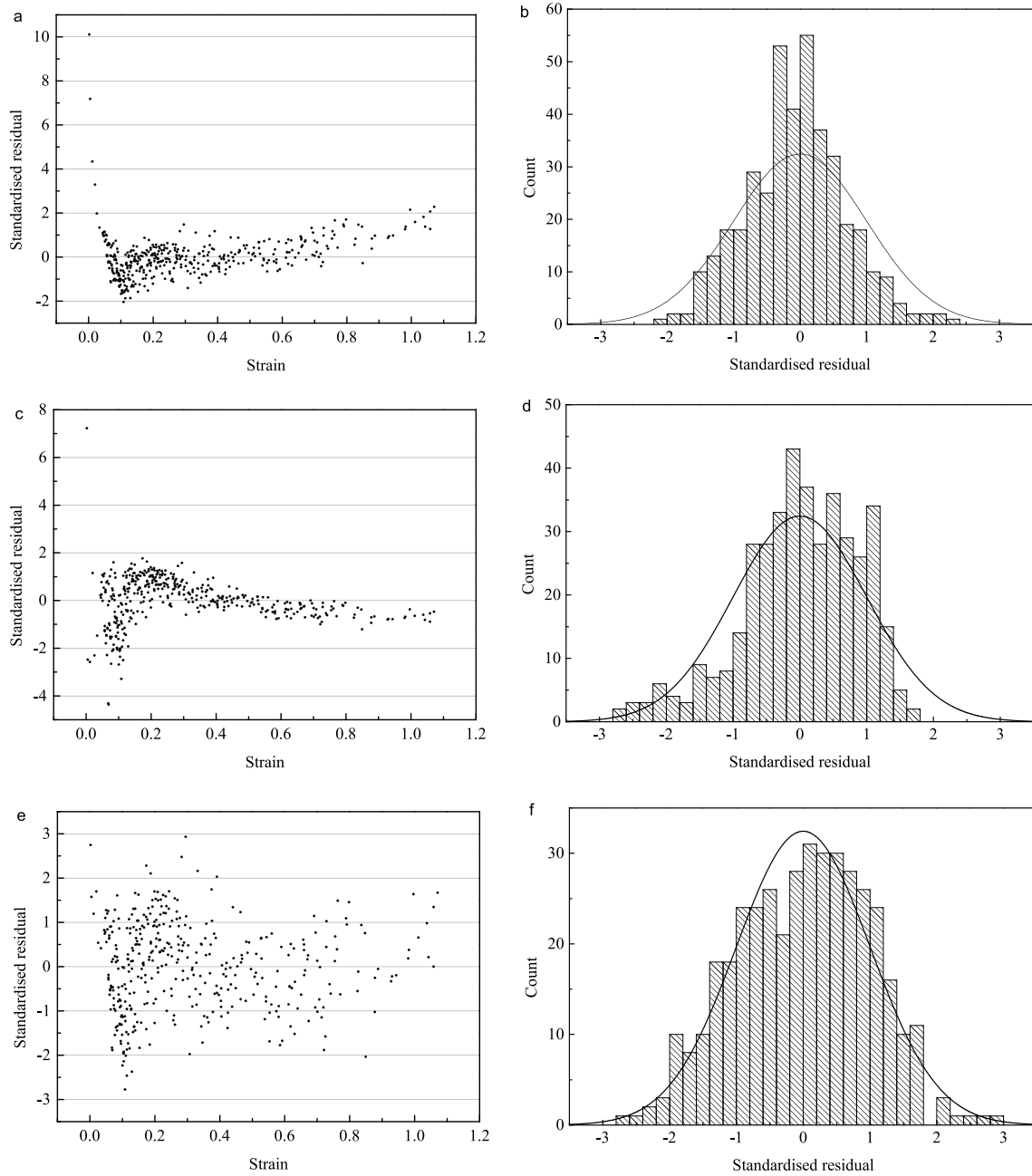


Figure 11 Normal frequency and distribution of residual for power regression equation: (a) Residual normal frequency of power function without constant, (b) Residual distribution of power function without constant, (c) Residual normal frequency of power function with initial hardness, (d) Residual distribution of power function with initial hardness, (e) Residual normal frequency of power function with initial fitting constant, (f) Residual distribution of power function with initial fitting constant

The outliers whose standardized residuals are outside the $(-2, 2)$ interval were eliminated according to Figure 11. The data eliminating outliers have been fitted by the three types of power functions, and the regression models can be expressed by Eqs. (22, 23, 24), where the initial hardness of the material is 180 HV. Compared

with Eqs. (19, 20, 21), only the fitting coefficients are slightly different.

$$H_{V, \text{powerF}} = 281.65e^{0.1463}, \tag{22}$$

$$H_{V,\text{powerS}} = 180 + 130.56\varepsilon^{0.7932}, \quad (23)$$

$$H_{V,\text{powerT}} = 284.64(\varepsilon + 0.098)^{0.2143}. \quad (24)$$

Similarly, the linearization and change of variable have been carried out for Eqs. (22, 23, 24), and then significance test for regression equation and regression coefficient were carried out. The results indicated that the multiple correlation coefficients R of the power regression equations are 0.9760, 0.9654 and 0.9847, which are all greater than the critical value R_α under $\alpha = 0.01$, and greater than the R of the corresponding regression equation before removing outliers. The variance ratios F of power regression equations after removing outliers are also much larger than the critical value F_α under $\alpha = 0.01$, and it is significantly greater than the corresponding F of regression equation before removing outliers. All these indicated that the significant of the power regression equation after removing outliers has been obviously improved.

The regression coefficient significance test was also carried out for linearized power regression models. The partial correlation coefficients of the independent variables for three linearized equations are 0.9760, 0.9654 and 0.9847, respectively, which are all greater than the corresponding V_j before removing outliers. The t -test with confidence level of $\alpha = 0.01$ also indicated that $|t_j|$ is also greater than corresponding $|t_j|$ before removing outliers, and is greater than the critical value. These indicated that the effect of independent variables of the power regression equation after removing outliers on the significance of the dependent variables has been obviously improved.

4.3 Evaluation and Application of Correlation Mode

4.3.1 Multi-pass PAE and Rolling Experiment

The single-pass and multi-pass PAE shown in Figure 3 were carried out with different reduction. The stroke (s) of upper die is 1 mm in single-pass PAE and is 2 mm in multi-pass PAE. In single-pass process, 100% of s_{single} was completed in one loading step. In multi-pass process, 0.5 mm reduction, i.e., 25% of s_{multi} , was performed for every loading step, and the unloading was carried out after every loading step. The FEAs of single and multi-pass PAEs were also carried out with the same processing parameters. After forming, to take a point on each of left and right tops, left and right flanks and center bottom for formed profile, and to take corresponding points below above 5 points, and thus 10 points have been selected from one workpiece of PAE, as shown in Figure 12(a).

The thread rolling process shown in Figure 1(b) was carried out on the servo-driven rolling equipment by developed by Xi'an Jiaotong University, and the pitch

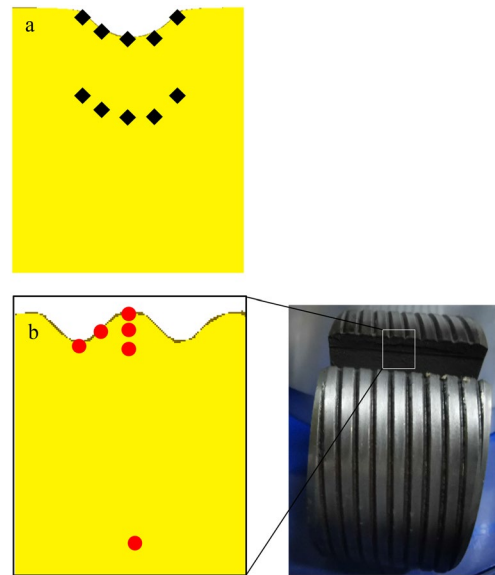


Figure 12 Schematic diagram of measurement-point position: (a) PAE, (b) Thread rolling test

diameter of the rolled thread was about 80mm. The detailed description about the rolling equipment can be found in the previous study [34–36]. Using the treatment of motion during rolling process [2, 32, 37], and considering the phase requirements of multi rolling dies before rolling [38], FEA of thread rolling was also carried out with the same processing parameters. Where, the material models and friction conditions described in Sections 2 and 3 were adopted. 3 points were taken on the crest, flank and root of rolled thread, and 3 points were taken from superficial layer to core, as shown in Figure 12(b).

The low-load Vickers hardness test for above 26 points from three workpieces were performed, equivalent strain information of corresponding points was also extracted from FEM results. Then, the data (i.e., testing samples or verifying samples) about hardness and strain for different deformation conditions besides training samples have been obtained, as shown in Figure 13. The equivalent strains of testing samples obtained from single and multi-pass PAEs are less than 1.2, and the equivalent strains of testing samples obtained from thread rolling are in the range of (0, 2.2).

4.3.2 Evaluation and Application

Figure 13(a) illustrates the curves of polynomial regression models Eqs. (14, 15, 16) and 26 testing samples. The predicting error of hardness by polynomial regression models is smaller when $\varepsilon < 1.2$ but is greater when $\varepsilon > 1.2$. The predicting error of hardness by polynomial

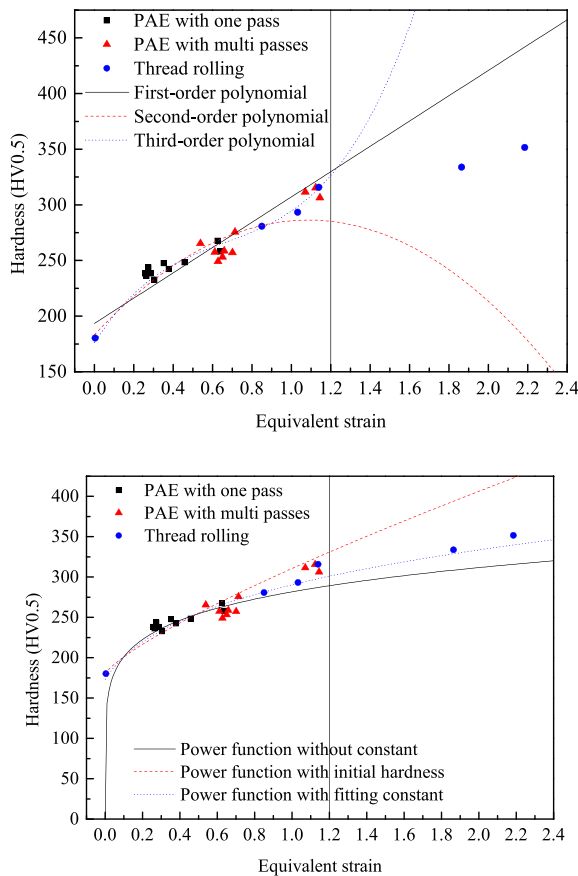


Figure 13 Different predicting models and experimental data with different forming conditions: (a) Polynomial, (b) Power function

regression models is less than 10% when strain is less than 1.2. However, is about 20%–165% when strain is greater than 1.2; and more the order of polynomial, the greater the error.

Figure 13(b) illustrates the curves of power regression models Eqs. (22, 23, 24) and 26 testing samples. Three types of power functions, such as without constant term, with the initial hardness as constant and with a fitting constant, can more reasonably describe the relationship between strain and hardness in a larger strain range. However, the power regression model (Eq. (22)) without a constant term is not suitable for describing the strain-hardness relationship under small strains. For example, the predicting error of hardness is as high as 30.32% for testing sample with $\epsilon = 0.004$ in the thread rolling process. The power regression model (Eq. (23)) with the initial hardness as constant term has poor extension, and the predicting error of hardness is about 20% when the strain is greater than 1.2.

In order to further quantitatively analyze the applicability of different regression models for the relationship

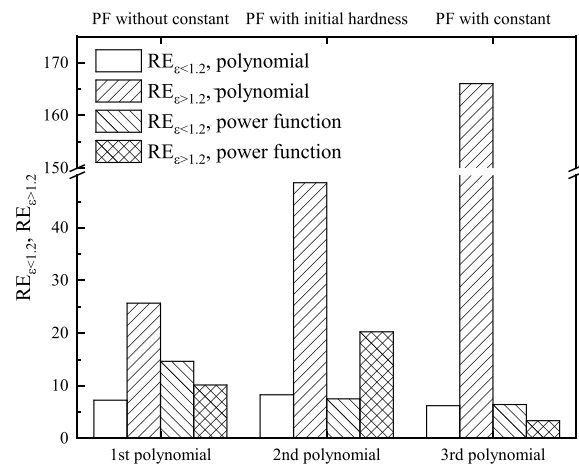


Figure 14 Predicting errors of different regression models

between strain and hardness, the predicting error $RE_{\epsilon < 1.2}$ of hardness by regression model under $\epsilon < 1.2$ is defined by Eq. (25); and $RE_{\epsilon > 1.2}$ of hardness by regression model under $\epsilon > 1.2$ is defined by Eq. (26).

$$RE_{\epsilon < 1.2} = \frac{RE_{\max}^{PAE1} + RE_{\max}^{PAE2} + RE_{\max, \epsilon < 1.2}^{Rolling}}{3}, \quad (25)$$

where RE_{\max}^{PAE1} and RE_{\max}^{PAE2} are the maximum of predicting error of regression model for testing samples obtained from single-pass PAE and multi-pass PAE, respectively; $RE_{\max, \epsilon < 1.2}^{Rolling}$ is the maximum of predicting error of regression model for testing samples obtained from thread rolling in the range of strain being less than 1.2.

$$RE_{\epsilon > 1.2} = RE_{\max, \epsilon > 1.2}^{Rolling}, \quad (26)$$

where $RE_{\max, \epsilon > 1.2}^{Rolling}$ is the maximum of predicting error of regression model for testing samples obtained from thread rolling in the range of strain being greater than 1.2.

Figure 14 illustrates the index RE for different regression models. When the strain is in the range of (0, 1.2), $RE_{\epsilon < 1.2}$ of polynomial regression model increases first and then decreases as the order increases; and the $RE_{\epsilon < 1.2}$ of the three types of power functions (PF) without constant terms, with initial hardness, and with fitting constant decreases in turn. The $RE_{\epsilon < 1.2}$ of polynomial regression model (Eq. (16)) with third-order is close to that of and the power regression model (Eq. (24)) with fitting constant. The polynomial regression model (Eq. (16)) with third-order has the smallest predicting error on hardness, which is about 6%. The average error of third-order polynomial regression model (Eq. (16)) for testing sample is also slightly smaller than that of power regression model (Eq. (24)). Thus,

prediction result of third-order polynomial regression model (Eq. (16)) is better than that of the other regression models when strain is in the range of (0, 1.2).

In the range of $\varepsilon > 1.2$, the $RE_{\varepsilon > 1.2}$ of polynomial regression model increases from first-order to third-order, and the $RE_{\varepsilon > 1.2}$ of the three types of power functions without constant terms, with initial hardness, and with fitting constant increases first and then decreases in turn. The polynomial regression models and the power regression model with initial hardness have a larger $RE_{\varepsilon > 1.2}$, so these regression models may be not suitable to describe the relationship between strain and hardness. The $RE_{\varepsilon > 1.2}$ of the power regression model (Eq. (22)) without constant term is about 10%, and the $RE_{\varepsilon > 1.2}$ of the power regression model (Eq. (24)) with fitting constant term is less than 5%.

According to the above analysis, the relationship between strain and hardness can be better described by third-order polynomial regression model (Eq. (16)) in the range of $\varepsilon < 1.2$ but by power regression model (Eq. (24)) with fitting constant in the range of $\varepsilon > 1.2$. Therefore, the relationship between strain and hardness in complex profile cold rolling of 45# steel can be described the segmented function (Eq. (27)). At the critical point $\varepsilon = 1.2$, the average value between the calculating value by third-order polynomial regression model (Eq. (16)) and the calculating value by power regression model (Eq. (24)) with fitting constant is adopted.

$$H_V = \begin{cases} 176 + 277.2\varepsilon - 319.9\varepsilon^2 + 161.1\varepsilon^3, & \varepsilon < 1.2 \\ 284.64(\varepsilon + 0.098)^{0.2143}, & \varepsilon > 1.2 \end{cases}, \quad (27)$$

where hardness is the average value of calculating values by polynomial and power regression models for critical $\varepsilon = 1.2$.

5 Conclusions

- (1) Based on the combination of PAE and FEA, the hardness data and corresponding strain data for cold rolling process of 45# steel were obtained. The data were analyzed by first to fourth-order polynomials and three power functions, and then the corresponding regression models have been established to describe the relationship between strain and hardness. The significance test of regression coefficient indicated that the first to third-order polynomials and the power functions without constant term, with initial hardness as constant term and with fitting constant term are suitable to describe the correlation between hardness and strain.

- (2) The testing samples were obtained from the single-pass and multi-pass PAEs and the thread rolling process, and then three polynomial regression models and three power regression models evaluated by the testing samples. The predicting error of hardness for polynomial regression models is less than 10% in the range of $\varepsilon < 1.2$, and the error is larger in the range of $\varepsilon > 1.2$. Compared with the polynomial regression model, the power regression model has better extension, and can better describe the relationship between the strain and the hardness outside (i.e., $\varepsilon > 1.2$) the training data range (i.e., $\varepsilon < 1.2$). Especially, the predicting error of power regression model with fitting constant is less than 5%.
- (3) The evaluation and application based on PAE and thread rolling process reflecting various complex profile rolling process indicated that the power regression model (Eq. (6)) without constant term is difficult to describe the relationship between strain and hardness under small strain, and the power regression model (Eq. (17)) with initial hardness has poor applicability outside the strain range of training samples; the third-order polynomial regression model (Eq. (16)) can better describe the relationship between strain and hardness in the range of $\varepsilon < 1.2$, while the power regression model (Eq. (24)) with fitting constant term is more suitable to describe the relationship between strain and hardness in the range of $\varepsilon > 1.2$.

Acknowledgements

Not applicable.

Authors' Contributions

DZ proposed the conception, designed the study and wrote the manuscript; LH performed the data analyses and draft preparation; BL performed the experiment and FEA; SZ supervised the study. All authors read and approved the final manuscript.

Authors' Information

Dawei Zhang, born in 1982, is currently a professor at *School of Mechanical Engineering, Xi'an Jiaotong University, China*. He received his PhD degree from *Northwestern Polytechnical University, China*, in 2012. His research interests include plastic forming technology and equipment, hydraulic system, tribology, etc.

Linghao Hu, born in 1997, received his master degree from *School of Mechanical Engineering, Xi'an Jiaotong University, China*, in 2022.

Bingkun Liu, born in 1995, received his master degree from *School of Mechanical Engineering, Xi'an Jiaotong University, China*, in 2020.

Shengdun Zhao, born in 1962, is currently a professor at *School of Mechanical Engineering, Xi'an Jiaotong University, China*. He received his PhD degree from *Xi'an Jiaotong University, China*, in 1997. His main research interests include plastic forming technology and equipment, computer control of mechanical-electrical-hydraulic system, fluid transmission and control, etc.

Funding

Supported by National Natural Science Foundation of China (Grant No. 51675415), and Key Research and Development Program of Shaanxi, China (Grant No. 2021GXJLH-Z-049).

Availability of Data and Materials

Data supporting results are included in this article.

Declarations

Competing Interests

The authors declare no competing financial interests.

Received: 25 August 2021 Revised: 11 August 2022 Accepted: 13 September 2023

Published online: 16 October 2023

References

- [1] D W Zhang. *Theory and technology of thread and spline synchronous rolling*. Beijing: China Science Publishing & Media Ltd., 2020. (in Chinese)
- [2] D W Zhang, D H Li, B K Liu, et al. Investigation and implementation for forming lead screw by through-feed rolling process with active rotation. *Journal of Manufacturing Processes*, 2022, 82: 96-112.
- [3] D W Zhang, Y T Li, J H Fu, et al. Mechanics analysis on precise forming process of external spline cold rolling. *Chinese Journal of Mechanical Engineering*, 2007, 20(3):54-58.
- [4] S W Zhang, D W Zhang, H Jiang, et al. Numerical and experimental analysis of deformation behaviors and microstructure evolution in the thread rolling process. *Journal of Materials Research and Technology*, 2022, 19: 230-242.
- [5] M C Cui, S D Zhao, C Chen, et al. The experimental study of axial in-feed incremental rolling process of spline shaft. *Journal of Mechanical Engineering*, 2018, 54(7): 199-204. (in Chinese).
- [6] J L Song, Z Q Liu, Y T Li. *Cold rolling precision forming of shaft parts: Theory and technologies*. Heidelberg: Springer-Verlag, 2017.
- [7] D W Zhang, F F Xu, Z C Yu, et al. Coulomb, Tresca and Coulomb-Tresca friction models used in analytical analysis for rolling process of external spline. *Journal of Materials Processing Technology*, 2021, 292:117059.
- [8] J P Domblesky, F Feng. Two-dimensional and three-dimensional finite element models of external thread rolling. *Proceedings of the Institution of Mechanical Engineers Part B*, 2002, 216: 507-517.
- [9] A A Kamouneh, J Ni, D Stephenson, et al. Investigation of work hardening of flat-rolled helical-involute gears through grain-flow analysis, FE-modeling, and strain signature. *International Journal of Machine Tools & Manufacture*, 2007, 47: 1285-1291.
- [10] F Chen, H Zhu, W Chen, et al. Multiscale modeling of discontinuous dynamic recrystallization during hot working by coupling multilevel cellular automaton and finite element method. *International Journal of Plasticity*, 2021, 145: 103064.
- [11] D Tabor. The hardness of solids. *Review of Physics in Technology*, 1970, 1(3): 145-179.
- [12] J R Cahoon, W H Broughton, A R Kutzak. The determination of yield strength from hardness measurements. *Metallurgical Transactions*, 1971, 2: 1979-1983.
- [13] J R Cahoon. An improved equation relating hardness to ultimate strength. *Metallurgical Transactions*, 1972, 3: 3040.
- [14] E J Pavlina, C J Van Tyne. Correlation of yield strength and tensile strength with hardness for steels. *Journal of Materials Engineering and Performance*, 2008, 17(6): 888-893.
- [15] I Brooks, P Lin, G Palumbo, et al. Analysis of hardness-tensile strength relationships for electroformed nanocrystalline materials. *Materials Science and Engineering A*, 2008, 491: 412-419.
- [16] J T Busby, M C Hash, G S Was. The relationship between hardness and yield stress in irradiated austenitic and ferritic steels. *Journal of Nuclear Materials*, 2005, 336: 276-278.
- [17] J H Kim, M Nakamichi. Effect of grain size on the hardness and reactivity of plasma-sintered beryllium. *Journal of Nuclear Material*, 2014, 456: 22-26.
- [18] G Z Voyiadjis, M Yaghoobi. Large scale atomistic simulation of size effects during nanoindentation: dislocation length and hardness. *Materials Science & Engineering A*, 2015 634: 20-31.
- [19] H Kim, S M Lee, T Altan. Prediction of hardness distribution in cold back extruded cups. *Journal of Materials Processing Technology*, 1996, 59: 113-121.
- [20] F O Sonmez, A Demir. Analytical relations between hardness and strain for formed parts. *Journal of Materials Processing Technology*, 2007, 186: 163-173.
- [21] B P P A Gouveia, J M C Rodrigues, P A F Martins. Finite element modeling of cold forward extrusion using updated Lagrangian and combined Eulerian- Lagrangian formulations. *Journal of Materials Processing Technology*, 1998, 80-81: 647-652.
- [22] R G Narayanan, M Gopal, A Rajadurai. Influence of friction in simple upsetting and prediction of hardness distribution in a cold forged product. *Journal of Testing and Evaluation*, 2008, 36(4): 1-13.
- [23] C H Chen, S T Wang, R S Lee, 2005. 3-D Finite element simulation for flat-die thread rolling of stainless steel. *Journal of the Chinese Society of Mechanical Engineers*, 2005, 26(5): 617-622.
- [24] D W Zhang, S D Zhao. Influences of friction condition and end shape of billet on convex at root of spline by rolling with round dies. *Manufacturing Technology*, 2018, 18(1): 165-169.
- [25] D W Zhang, M C Cui, M Cao, et al. Determination of friction conditions in cold-rolling process of shaft part by using incremental ring compression test. *The International Journal of Advanced Manufacturing Technology*, 2017, 91: 3823-3831.
- [26] D W Zhang, Z J Li, G C Yang, et al. Research progresses of description and evaluation for friction during bulk metal forming. *Forging & Stamping Technology*, 2021, 46(10): 1-11. (in Chinese)
- [27] C Chen, Y X Li, Z Y Zhai, et al. Comparative investigation of three different reforming processes for clinched joint to increase joining strength. *Journal of Manufacturing Processes*, 2019, 45: 83-91.
- [28] D W Zhang, X G Fan. Review on intermittent local loading forming of large-size complicated component: deformation characteristics. *The International Journal of Advanced Manufacturing Technology*, 2018, 99: 1427-1448.
- [29] D W Zhang, B K Liu, J X Li, et al. Variation of friction conditions in cold ring compression tests of medium carbon steel. *Friction*, 2020, 8(2): 311-322.
- [30] D W Zhang, G C Yang, S D Zhao. Frictional behavior during cold ring compression process of aluminum alloy 5052. *Chinese Journal of Aeronautics*, 2021, 34(5): 47-64.
- [31] D W Zhang, G C Yang, Z B Zheng. Effect of forming conditions on frictional characteristic in cold bulk forming process of copper alloy. *Tribology International*, 2021, 155: 106786.
- [32] D W Zhang, C Zhang, C Tian, et al. Forming characteristic of thread cold rolling process with round dies. *The International Journal of Advanced Manufacturing Technology*, 2022, 120: 2503-2415.
- [33] M C Cui, S D Zhao, D W Zhang, et al. Deformation mechanism and performance improvement of spline shaft with 42CrMo steel by axial-infeed incremental rolling process. *The International Journal of Advanced Manufacturing Technology*, 2017, 88: 2621-2630.
- [34] S D Zhao, X Jia. Research progress and development trend of intelligent manufacturing and its core information equipment. *Mechanical Science and Technology for Aerospace Engineering*, 2017, 36(1): 1-16. (in Chinese)

- [35] H X Sun, M C Cui, Y S Zhang, et al. Performance of AC servo axial-infeed incremental warm rolling equipment and simulated production of spline shafts. *The International Journal of Advanced Manufacturing Technology*, 2018, 94: 2089-2097.
- [36] D W Zhang, S D Zhao, L M Wang. Current status of rolling forming machine for complex profile. *Journal of Netshape Forming Engineering*, 2019, 11(1): 1-10. (in Chinese).
- [37] D W Zhang. *Modeling, simulation and application for bulk metal forming process*. Beijing: China Science Publishing & Media Ltd., 2022. (in Chinese)
- [38] D W Zhang, B K Liu, F F Xu, et al. A note on phase characteristic among rollers before thread or spline rolling. *The International Journal of Advanced Manufacturing Technology*, 2019,100: 391-399.

Submit your manuscript to a SpringerOpen[®] journal and benefit from:

- ▶ Convenient online submission
- ▶ Rigorous peer review
- ▶ Open access: articles freely available online
- ▶ High visibility within the field
- ▶ Retaining the copyright to your article

Submit your next manuscript at ▶ [springeropen.com](https://www.springeropen.com)
